DNA Condensation by PAMAM Dendrimers: Self-Assembly Characteristics and Effect on Transcription[†]

Kristina Fant, Elin K. Esbjörner, Per Lincoln, and Bengt Nordén*

Department of Chemical and Biological Engineering/Physical Chemistry, Chalmers University of Technology, SE-412 96 Gothenburg, Sweden

Received August 23, 2007; Revised Manuscript Received November 16, 2007

ABSTRACT: Electrostatic shielding and steric blocking by histones are two significant factors that participate in the control of the local rates of transcription in chromatin. As a simple model system to determine how the degree of DNA condensation affects enzyme accessibility and gene expression, we have used generation 5 polyamidoamine (G5 PAMAM) cationic dendrimer particles (size 5.4 nm) as a synthetic histone model together with an *in vitro* transcription assay. The degree of compaction, conformation, and binding availability of the dendrimer−DNA complexes is characterized by linear and circular dichroism, dynamic light scattering, and competitive binding of ethidium. Using ultracentrifugation we are able to show explicitly, for the first time, that dendrimer particles bind to DNA in a highly cooperative manner, and that the dendrimer-induced condensation of the DNA strongly attenuates transcription. Two fractions with different properties can be identified: a low-density fraction which behaves very similar to uncondensed DNA and a high-density fraction which is condensed to a high extent and where binding availability and transcription are strongly reduced. Circular dichroism gives clues to the structure of the condensed DNA indicating long-range order between the helices such as in polymer-salt-induced cholesteric liquid crystalline domains, one possible shape being a toroidal structure. On the basis of the experimental data, we propose a model for the self-assembly of the dendrimer−DNA system.

In the nucleus of a eukaryotic cell, the vast amount of DNA is organized by wrapping around histone proteins forming the well-characterized nucleosome core particle (*1*). Together with other proteins, nucleosome core particles are in turn folded into more or less condensed structures depending on the local environment. These structures, collectively known as chromatin, not only allow the genome to be contained in the small volume of the nucleus; chromatin also has a regulatory function on the level of gene expression where more condensed regions are much less expressed than loosely condensed ones (*2*). The degree of condensation of the DNA in chromatin is impressive; the volume of the DNA is reduced more than 10 000 times inside the nucleus (*3*). *In vitro* DNA condensation can be achieved by a variety of natural or synthetic cationic agents such as multivalent ions (*4*, *5*), lipids (*6*), and linear, branched, or dendritic polymers (*7*, *8*). This area has been extensively explored due to the possible applications of condensed DNA in nonviral gene delivery (*9*). Further, the study of DNA condensation in simple model systems is pursued to give deeper insights into the *in vivo* effect of condensation and the energetics governing this process (*10*).

Polyamidoamine (PAMAM[1]) dendrimers are branched cationic polymers and have been used successfully for delivery of plasmid DNA as well as oligonucleotides to a variety of cell types with high efficiency *in vitro* (*11*−*15*). They can easily be modified, and recently functionalized PAMAM dendrimers have been used for gene delivery *in vivo* into kidney (*16*) and brain (*17*) tissue of mice. Because of their well-defined size and surface charge density as well as the possibility to synthetically tune both these properties, PAMAM dendrimers are well suited as artificial histone-mimicking agents and highly useful for studying, in simple models, what influences the structure of polymer−DNA complexes and how the complex structure is related to the biological function of the DNA. Several groups have undertaken biophysical characterization of dendrimer−DNA complexes (*18*−*24*), showing that the nature of interaction is primarily electrostatic and that higher ionic strength due to screening effects decreases dendrimer−DNA affinity. Upon binding, DNA is condensed to varying degrees depending on dendrimer generation (size) and charge ratio (i.e., amount of positive amines on the dendrimer over negative phosphates on the DNA, [N]/[P]). The most efficient transfection is seen for intermediate to higher generation dendrimers (generations 5−8) used at charge ratios 5−10 (large excess of dendrimers). At these charge ratios DNA is effectively protected from nucleases, and despite successful transcription *in vivo*, inhibition of *in vitro* transcription has been demonstrated (*19*). In electron microscopy, a largely heterogeneous complex population of dendrimer−DNA complexes, ranging from compact spherical or toroidal structures to very large (1−2 μm) irregular aggregates can be observed. Successful attempts to modulate the size of

[†] This work was supported by funding from the EU 6th framework program, contract No. 012967.

* Corresponding author. Phone: +46 31 7723041. Fax: +46 31 7723858. E-mail: norden@chembio.chalmers.se.

[1] Abbreviations: PAMAM, polyamidoamine; LD, linear dichroism; CD, circular dichroism; DLS, dynamic light scattering; EtBr, ethidium bromide.

10.1021/bi7017199 CCC: $40.75
Published on Web 01/12/2008

DNA−dendrimer complexes have been made using either partially fractured dendrimers (*18*) or by inclusion of small anionic molecules such as DNA oligomers or sulfate dextran (*12*, *25*), resulting in a more homogeneous population of smaller particles which also display increased transfection efficiency.

Despite the relatively large number of publications on DNA and dendrimers, few studies concern dendrimer-induced DNA condensation at low charge ratios (<1). We seek to understand how DNA condensation affects gene expression, and since the nucleosome core particles have an excess negative charge (*3*) this is the relevant domain to investigate. Using a simple system consisting of PAMAM dendrimers and linear DNA of uniform length, we examine what level of condensation is required in order to turn off transcription *in vitro*. Preliminary results showed no effect on transcription for charge ratios <1. This led us to suspect that the dendrimers bound cooperatively to DNA, which would result in essence in the presence of two fractions: one condensed DNA fraction and one fraction of effectively totally uncondensed DNA. As the uncondensed DNA would be readily transcribed this would shadow the effect of DNA condensation and explain our results. To test this, we have employed ultracentrifugation as a method to separate the two fractions. Our results confirm the hypothesis, and in this paper we are able to show explicitly, for the first time, that dendrimers bind to DNA in a cooperative manner. The dendrimer-induced condensation of the DNA does influence the degree of transcription in an *in vitro* system Using LD, CD, dye exclusion, and DLS we have been able to characterize the structure and degree of condensation of the DNA in the two fractions. On the basis of the experimental data, we propose a model for the self-assembly of the dendrimer−DNA system.

MATERIALS AND METHODS

Materials. Generation 5 polyamidoamine (PAMAM) dendrimers ($C_{1262}H_{2528}N_{506}O_{252}$), synthesized as previously described (*26*) and characterized by ^1H and ^{13}C NMR, was a kind gift from Dr. M.C. Grossel, Southampton University, U.K. They were stored in water at a concentration of 0.18 mM and were further diluted at need depending on the volume of DNA used. Luciferase T7 Control plasmid (Promega), a 4331 bp plasmid encoding the luciferase gene under control of the T7 promotor, was amplified in *E. coli* strain *Top10* and purified using a QIAfilter Plasmid Giga Kit (Qiagen). *In vitro* transcription was assessed using the commercially available TNT Coupled Reticulocyte Lysate System (Promega). All DNA and ethidium bromide (EtBr) concentrations were determined by absorbance using a Varian Cary 4000 UV−vis spectrophotometer (Varian Inc) and extinction coefficients $\epsilon_{260} = 6600\ M^{-1}\ cm^{-1}$ for DNA and $\epsilon_{476} = 5680\ M^{-1}\ cm^{-1}$ for EtBr. The buffer used contained 20 mM HEPES and 150 mM NaCl (pH 7.4).

Plasmid DNA Preparation. The Luciferase T7 Control DNA plasmid was amplified in *E. Coli* strain *Top10* according to standard procedures (*27*). The bacteria were harvested, and the plasmid DNA was purified using a QIAfilter Plasmid Giga Kit (Qiagen) according to the manufacturer's instructions. The intactness and identity of the plasmid was confirmed by agarose gel electrophoresis. For linearization, the plasmid DNA was digested with Pdm1 (Fermentas). The efficiency of the reaction was 100% as confirmed by agarose gel electrophoresis. To remove the restriction buffer, the linearized DNA was precipitated using 2-propanol, centrifuged, washed once with 70% ethanol, and resuspended in 20 mM HEPES with 10 mM NaCl. The plasmid stock solution was stored at −20 °C. For each new experiment, an aliquot of DNA was thawed and diluted to 100 μM in 20 mM HEPES with 150 mM NaCl (pH 7.4).

Complex Preparation. Dendrimer−DNA complexes were formed by adding a small volume (1−5 μL) from a G5 PAMAM dendrimer stock solution to a 100 μM DNA solution. For *in vitro* transcription−translation experiments, a 300 μM DNA solution was used. The complexes form instantaneously at room temperature and the incubation time prior to experiments was 10 min. Complexes with varying dendrimer−DNA ratios were formed, and the composition of the complexes will hereafter be characterized by the charge ratio, r, of positive amine groups on the dendrimer surface to negative phosphate groups on the DNA. At pH 7.4, the dendrimers are supposed to be fully protonated so that each dendrimer has 128 positive charges. In this study, two types of experiments were performed: Either DNA was titrated with small volumes of dendrimer stock solution to assess the effect of varying dendrimer−DNA ratios, or samples were prepared by ultracentrifugation of a dendrimer−DNA solution with $r = 0.5$, after which both supernatant and pellet were recovered (vide infra). The samples were analyzed by spectroscopic techniques as described below. Samples for the *in vitro* transcription−translation experiments were prepared separately with special precautions to avoid RNase contamination (vide infra).

Ultracentrifugation. Low- and high-density dendrimer−DNA complexes were separated using ultracentrifugation at 79500*g* for 20 min in a Beckman−Coulter Optima 40-K ultracentrifuge with a Ti 70.1 rotor. The pellet was recovered by carefully rinsing the centrifuge tubes with buffer. For the *in vitro* transcription assay, the centrifuge tubes were washed with RNaseZap (Sigma), rinsed carefully with RNase-free water and air-dried before use to avoid RNase contamination.

Flow Linear Dichroism Spectroscopy. Linear dichroism (LD) is defined as the difference in absorbance of linearly polarized light parallel and perpendicular to a macroscopic orientation axis (*28*) and was here used to assess the degree of orientation of DNA in absence and presence of dendrimers. Samples with DNA and dendrimers were oriented in a Couette flow cell with an outer rotating cylinder using a shear gradient of 3100 s^{-1}. All measurements were performed on a Jasco J-720 CD spectropolarimeter equipped with an Oxley prism to obtain linearly polarized light (*28*). Spectra were recorded from 220 to 350 nm in 1 nm increments at ambient temperature and baseline-corrected by subtraction of a spectrum recorded on the nonoriented sample.

Circular Dichroism Spectroscopy. Circular dichroism (CD) is defined as the difference in absorbance of left and right circularly polarized light and was here used to assess how the DNA secondary structure is affected by dendrimer binding. All CD measurements were performed on a Jasco J-810 spectropolarimeter at 25 °C using a 1 cm quartz cell. Spectra were recorded in 1 nm increments from 220 to 400 nm and baseline-corrected by subtracting appropriate blanks.

The bandwidth was set to 1 nm, the response was 0.5 s, and the scan speed was 50 nm/min. Ten scans were accumulated and averaged.

Dynamic Light Scattering. Dynamic light scattering (DLS) measurements were performed on an ALV CGS-8F DLS/SLS-5022F instrument (ALV, Germany), equipped with an ALV-6010/160 correlator and dual APD detectors, at 25 °C. The wavelength of the incident light was 632.8 nm, and the scattering angle was set to 90°. Data were collected for a period of 300 s. The decay time distribution was obtained from the autocorrelation function, and the average hydrodynamic radius was calculated using second-order cumulant analysis.

Binding Isotherms for Ethidium Bromide. The binding efficiency of the monovalent cation ethidium to compacted DNA was determined by recording emission spectra of ethidium upon titration of dendrimer−DNA samples of known concentration with small volumes of EtBr. Typically, 10 μM of DNA (or dendrimer−DNA complexes) in 2 mL of buffer was titrated with aliquots of 2.5−10 μL 200 μM EtBr. Emission spectra were recorded from 550 to 700 nm using an excitation wavelength of 530 nm on a Varian Eclipse spectrofluorimeter (Varian Inc.). The excitation and emission bandpass was 5 and 10 nm, respectively. The amount of bound and free ethidium in each titration point was determined by least-squares projection of the measured spectra onto reference spectra corresponding to completely bound and completely free ethidium. Reference spectra were recorded in separate experiments, and that for completely bound ethidium was measured on a sample where a 60-fold excess of DNA was added to a 5 μM EtBr solution. The titration data, in the form of Scatchard plots, were fit to the McGhee and von Hippel conditional probability model of excluded site binding according to eq 1 (*42*)

$$\frac{\theta_{\mathrm{EtBr}}}{c_{\mathrm{f}}} = K_{\mathrm{EtBr}}(1 - s\theta_{\mathrm{EtBr}})\left[\frac{(1 - s\theta_{\mathrm{EtBr}})}{(1 - (s-1)\theta_{\mathrm{EtBr}}}\right]^{(s-1)} \quad (1)$$

with K_{EtBr} the apparent binding constant of ethidium to DNA and s the apparent binding site size. The parameter θ_{EtBr}, the ratio of bound ethidium to the number of DNA base pairs, was modified according to eq 2 by introducing a parameter x representing the apparent accessible fraction of binding sites on DNA remaining after dendrimer binding.

$$\theta_{\mathrm{EtBr}} = \frac{c_{\mathrm{b}}}{x c_{\mathrm{DNA}}} \quad (2)$$

The size of the binding site for ethidium on DNA (s) was calculated to 2.5 base pairs using titration data for uncondensed DNA. It was assumed that s does not change significantly upon dendrimer binding; hence, this value was kept constant for the remaining titration data where only values of K_{EtBr} and x were calculated.

In Vitro Transcription and Translation Using T7 Polymerase. The effect on transcription of compacting DNA with dendrimers was evaluated by assessing the *in vitro* synthesis of luciferase protein using a commercial coupled transcription−translation assay (TNT Coupled Reticulocyte Lysate System, Promega Inc., Madison, WI). The Luciferase T7 Control plasmid contains the luciferase gene under control of the T7 promotor. Plasmid DNA was preincubated with dendrimers in 10 μL of buffer (20 mM HEPES, 150 mM NaCl, pH 7.4) and added to 40 μL of the reaction mixture, which contains necessary nucleotides, amino acids, enzymes, and cofactors. The amount of produced luciferase in each reaction was assessed at different time points throughout the incubation by measuring the light intensity from luciferase when 2.5 μL aliquots were added to 60 μL of luciferin substrate (Luciferase Assay Reagent, #E1483, Promega). The chemoluminescence was monitored for a period of at least 60 s starting 30 s after addition of substrate using the detection system of a SPEX Fluorolog τ-3 spectrofluorimeter (JY Horiba) with the emission monochromator set at 0 nm to pass on all emitted light.

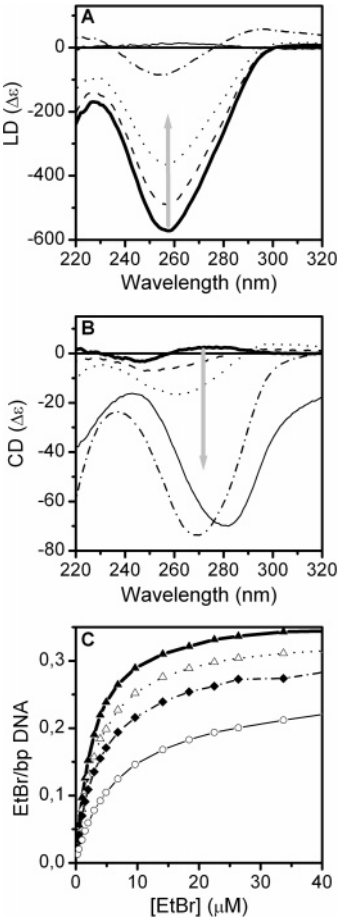

FIGURE 1: Characteristics of dendrimer−DNA complexes as a function of charge ratio (r). (A) Degree of DNA compaction assessed by flow linear dichroism (LD) of the DNA-base absorption band, (B) DNA conformation assessed by CD, and (C) binding isotherms of ethidium cation to condensed DNA determined by emission measurements. Data in A−C correspond to free DNA (thick solid line or ▲), $r = 0.2$ (dashed line); $r = 0.5$ (dotted line or △); $r = 1$ (dash-dot line or ◆); $r = 1.5$ (thin solid); and $r = 2$ (○).

RESULTS

Efficiency of DNA Condensation by Dendrimers. The condensation of linearized plasmid DNA by dendrimers was investigated using LD and CD spectroscopy, and titration with EtBr (Figure 1). The LD spectra (Figure 1A) show that the DNA band at 260 nm subsequently disappears with increasing charge ratio ([+]/[−]), and at charge ratios above 1.5 no signal is observed. This is because the orientation of the DNA in the flow cell is attenuated when all long stretches of DNA disappear as the DNA becomes condensed. The CD

Table 1: Apparent Binding Constants (K_{EtBr}) and Apparent Remaining Fraction of Binding Sites after DNA Condensation (x) for Ethidium Bound to Dendrimer/DNA Complexes of Varying Charge Ratios

	$K_{EtBr} \times 10^{-6}$ (M^{-1})[a]	x (% remaining binding sites)[a,b]
uncondensed DNA	0.31 ± 0.03	100
$r = 0.5$	0.17 ± 0.03	97 ± 1
$r = 1$	0.13 ± 0.03	91 ± 1
$r = 2$	0.05 ± 0.005	82 ± 3

[a] Reported values are the average of two to three independent experiments. [b] The binding site size was estimated to 2.5 base pairs (see Materials and Methods).

spectra of uncondensed DNA (thick solid line in Figure 1B) shows, as expected, a typical B-form signature with a positive peak at 274 nm, a negative peak at 246 nm, and a crossover near 260 nm. Upon condensation by dendrimers, a dramatic change in the CD spectra can be observed (dashed, dotted, and dash-dot lines in Figure 1B) resulting in complete disappearance of the positive peak at 274 nm and a significant red-shift and increase in magnitude of the negative peak. This is observed already for the lowest charge ratio investigated, and the negative peak increases in magnitude with increasing dendrimer concentration up to charge neutrality. At a charge ratio of 1.5, the CD minimum is red-shifted further and the baseline becomes tilted, indicating light scattering effects due to formation of larger particles (thin solid line in Figure 1B). The change in CD below charge neutrality closely resembles that of a polymer−salt-induced (Ψ) form of DNA, attributed to the formation of a liquid crystalline phase with parallel DNA helices in each layer (*29*−*31*, *36*). A Ψ-type CD spectrum has to our knowledge not previously been reported at this relatively low ionic strength (150 mM), or for dendritic polymers. This transition is not observed with supercoiled (circular) T7 plasmid DNA, nor at lower ionic strength (10 mM) or with longer, polydisperse DNA (calf thymus DNA) (data not shown).

The titrations of condensed DNA with EtBr show that dendrimers prohibit the cationic dye from binding to DNA (Figure 1C). As expected, increasing amounts of ethidium was excluded from the DNA when the charge ratio of dendrimer−DNA was increased from 0.5 up to 2. Higher charge ratios than 2 (3 and 10) were tried but did not result in further exclusion of ethidium (data not shown). Thus, for a small intercalator such as ethidium, dendrimers cannot make all binding sites on the DNA inaccessible, and a significant fraction is still available. This indicates a porous complex structure, where the smaller ethidium cation can diffuse and find free binding sites in between the dendrimers. This hypothesis is further supported by the calculated apparent binding constants (K_{EtBr}) and remaining fraction of binding sites (x) following DNA condensation (Table 1) determined as described in Materials and Methods by fitting the titration data to a modified version of the theoretical expressions for the McGhee and von Hippel conditional probability model of excluded site binding. The apparent accessible fraction of binding sites for ethidium is shown to only decrease moderately with increasing charge ratio, as would be expected for a porous dendrimer−DNA complex structure. The apparent binding constant for the dye, on the other hand, decreases considerably with increasing charge ratio. This is expected as the ethidium cation has to bind in between highly cationic dendrimer molecules whose electrostatic repulsion will reduce the affinity.

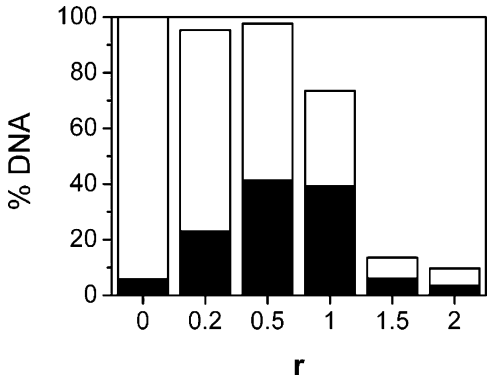

FIGURE 2: Percentage of DNA, in supernatant (white) and pellet (black) fractions collected after ultracentrifugation at 79300*g* for 20 min as a function of charge ratio (r). Data represents the average of five independent experiments. The mean standard deviation was 9% and the maximum standard deviation was 16% (for $r = 0.5$).

Ultracentrifugation of Condensed DNA. The binding of dendrimers to DNA was further investigated by separating condensed DNA into two fractions using ultracentrifugation. The centrifugal force was established experimentally as the highest possible force where the uncondensed DNA still remained in the supernatant (data not shown). The distribution of DNA between the supernatant and the pellet fractions was determined by absorption spectroscopy and is shown as a function of charge ratio in Figure 2. The amount of DNA in the supernatant decreased gradually with increasing charge ratio, and above charge neutrality almost no DNA was present. In the pellet, the amount of DNA was largest for charge ratios 0.5 and 1, while it was not possible to redissolve the entire pellet for charge ratios 1.5 and 2 even after extensive vortexing of the sample. Thus the total amount of DNA recovered after centrifugation was lower for charge ratios 1−2. The gradual decrease in DNA content in the supernatant with increasing charge ratio, as opposed to an abrupt decrease at $r = 1$, is indicative of a cooperative binding process (*29*). The fact that the pellet cannot be completely redissolved at charge ratios above 1 points toward the formation of some very large insoluble aggregates when DNA is overcharged.

Degree of Condensation in Supernatant and Pellet Fractions of Ultracentrifuged DNA. At charge ratio 0.5, the DNA is approximately equally distributed in the supernatant and pellet fractions after ultracentrifugation (Figure 2). The different degrees of condensation of the DNA in these fractions were investigated by LD, CD, and EtBr titration experiments (Figure 3) as well as by DLS (Figure 4). The LD spectra (Figure 3A) show that the DNA in the supernatant has a similar degree of orientation as uncondensed DNA, indicating that none or insignificant amounts of dendrimers have associated to this fraction of DNA. By contrast, the DNA in the pellet fraction displays a poor orientation (low LD) indicating a high degree of condensation, comparable to that at a charge ratio of 1 (Figure 1A). The LD spectra for pellet fractions were somewhat distorted, with tilted baselines and peak broadening, indicating presence of polarized light scattering. Likewise, the CD spectra (Figure 3B) show that the DNA in the supernatant fraction is typical

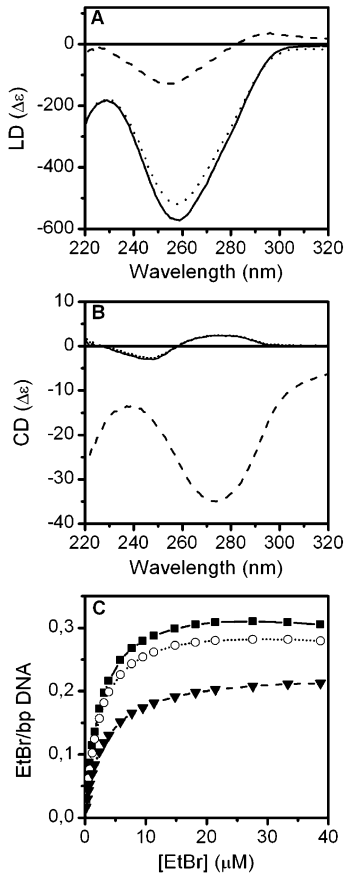

FIGURE 3: LD spectra (A) and CD spectra (B) of DNA compacted with dendrimers at a charge ratio of 0.5, recorded after separation of differently condensed fractions using ultracentrifugation. Data are shown for the supernatant fraction (dotted line), the redissolved pellet fraction (dashed), and as control spectra also for dendrimer-free DNA (solid line). The actual distribution of DNA between supernatant and pellet was approximately 50/50. (C) Binding isotherms for the association of EtBr to DNA in the supernatant fraction (○), the pellet fraction (▼), and to uncondensed dendrimer-free DNA (■).

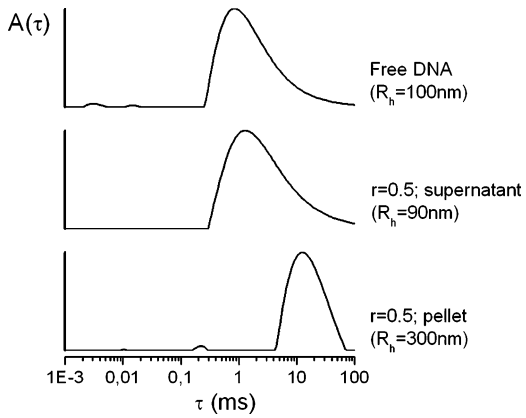

FIGURE 4: Relaxation time distributions $A(\tau)$ obtained by dynamic light scattering, for DNA compacted with dendrimers at a charge ratio of 0.5 and separated into two fractions using ultracentrifugation. Data for dendrimer-free DNA is shown for comparison. The reported values for the average hydrodynamic radius were calculated using second-order cumulant analysis assuming spherical particles.

B form, displaying exactly the same shape as uncondensed DNA, while the DNA in the pellet fraction gives rise to a Ψ-form CD signal, similar to what was earlier observed for dendrimer−DNA charge ratios above 1 (Figure 1B). The EtBr binding isotherms (Figure 3C) show that the DNA in the supernatant fraction is essentially as available to ethidium as free DNA whereas ethidium binding to the pelleted fraction is significantly reduced. Table 2 shows the apparent binding constant (K_{EtBr}) and the accessible fraction of binding sites (x) for ethidium, calculated as described in Materials and Methods assuming a constant binding site size (s) of 2.5. K_{EtBr} for the DNA in the supernatant is almost identical to K_{EtBr} for uncondensed, dendrimer-free DNA, while K_{EtBr} for the DNA in the pellet fraction is smaller. Similarly, the remaining fraction of binding sites in the supernatant fraction is 91%, while 71% in the pellet fraction. A comparison with Table 1 shows that the DNA in the pellet fraction has similar K_{EtBr} and x as DNA condensed to charge ratios 1−2.

Table 2: Apparent Binding Constants (K_{EtBr}) and Apparent Remaining Fraction of Binding Sites after DNA Condensation (x) for Ethidium Bound to Differently Condensed DNA in Supernatant and Pellet Fractions of Ultracentrifuged Dendrimer/DNA Complexes with Charge Ratio 0.5

	$K_{EtBr} \times 10^{-6}$ $(M^{-1})^a$	x (% remaining binding sites)^{a,b}
uncondensed DNA (control)	0.31 ± 0.03	100
supernatant fraction	0.30 ± 0.02	91 ± 1
pellet fraction	0.21 ± 0.01	71 ± 8

[a] Reported values are the average of two to three independent experiments. [b] The binding site size was estimated to 2.5 base pairs (see Materials and Methods).

The DLS experiments (Figure 4) show that the supernatant fraction displays approximately the same decay time distribution as dendrimer-free DNA, while the distribution for the pellet fraction is shifted toward longer decay times. This indicates formation of large aggregates in the pellet fraction, and the estimated hydrodynamic radii (R_H) of these complexes (indicated in Figure 4) suggests that several DNA strands are involved in each condensed particle rather than that the condensed DNA should be monomolecular. The apparent mean hydrodynamic radius is about 3-fold larger in the pellet fraction as compared to the supernatant fraction and uncondensed DNA.

Taken together, the LD, CD, and ethidium binding experiments as well as the DLS data indicate that the DNA in the pellet fraction is condensed to a much higher degree than the DNA in the supernatant fraction, which is essentially unaffected by dendrimers. This strongly points to a high degree of cooperativity in dendrimer-induced DNA condensation, an observation we shall return to in the Discussion.

Effect of DNA Condensation on in Vitro Transcription. The effect on *in vitro* transcription of condensing DNA with dendrimers was assessed by separating intermediately condensed linearized T7 plasmid DNA (charge ratio 0.5) into two fractions using ultracentrifugation as described above, and comparing the *in vitro* luciferase production from these two fractions. The results, which are shown in Figure 5, show that the DNA in the supernatant fraction is as accessible as the uncondensed DNA, while the DNA in the pellet fraction exhibits significantly reduced and delayed transcription/translation. It has been demonstrated that dendrimers do not stop the T7 RNA polymerase once transcription has been initiated, but only hinder the formation of the transcriptional complex (*19*). Therefore we believe that the reduced production of luciferase in the pellet fraction is a consequence of

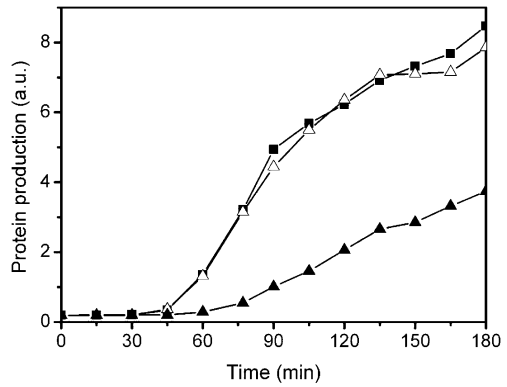

FIGURE 5: Transcription activity of the luciferase gene in linearized T7 plasmid DNA measured as the amount of produced protein as a function of time after addition of DNA to the reaction mixture. Transcription activity was assessed for the supernatant (△) and pellet (▲) fractions collected after ultracentrifugation of a DNA sample compacted with dendrimers at a charge ratio of 0.5. The transcription activity for dendrimer-free uncondensed DNA (■) is shown for comparison. The total DNA amount in each sample was 600 ng.

efficient condensation of DNA by the dendrimers, leading to reduced availability for transcription enzymes.

DISCUSSION

To obtain deeper understanding of the importance of DNA condensation for regulation of gene expression in the nucleus of eukaryotic cells, we have investigated the effect on *in vitro* transcription of condensing DNA with PAMAM dendrimers. We investigate how the level of condensation of the DNA affects the expression of a gene, and whether non-sequence-specific condensation is sufficient for silencing. Our results clearly show that there is a great difference in the amount of transcription between condensed and uncondensed DNA. Further, we have found that in our model system with dendrimers as "artificial histones", dendrimers are found to bind to DNA in a highly cooperative manner, i.e., they bind close to each other on the DNA. This implies that certain fractions of DNA are crowded with dendrimers while others are empty.

The stepwise decrease in DNA content in the supernatant with increasing r following ultracentrifugation shown in Figure 2 is an indirect proof for cooperative binding (*29*). This result contrasts to that of Bielinska et al., who found an abrupt decrease at charge neutrality for G5 PAMAM dendrimers complexed to herring sperm DNA (*20*). The dissimilarity can be explained by different ionic strengths: Bielinska et al. prepared the dendrimer−DNA complexes in distilled water whereas in this study the complexes were prepared in the presence of 150 mM NaCl. Since the interactions between dendrimers and DNA are primarily electrostatic, they should be greatly influenced by the presence of counterions. Switching between cooperative and noncooperative binding modes for a polylysine−DNA system at different ionic strengths has also been reported by Weiskopf et al. (*29*). Explicit proof for cooperative binding of dendrimers to DNA is obtained from this study through the separation of two fractions of differently condensed DNA at intermediate charge ratios (<1), followed by extensive characterization of the properties of the DNA in these fractions (Figures 3 and 4). The DNA in the supernatant fraction is very similar to uncondensed DNA, while the DNA in the redissolved pellet fraction resembles dendrimer-condensed DNA at higher charge ratios. A comparison between Figure 1A and Figure 3A shows that the LD signal for the pellet fraction of $r = 0.5$ is very similar to the LD signal for $r = 1$ in unfractionated dendrimer−DNA samples. Since the DNA is equally distributed in the supernatant and pellet fractions at $r = 0.5$, this is indeed the expected result if there is a high degree of cooperativity. The supernatant fraction contains virtually no dendrimers; therefore, the pellet fraction will effectively consist of a dendrimer−DNA mixture with approximately the same amount of charges. This distribution is formed spontaneously in the self-assembly of the system. Since the complexes stay in solution, they are likely to have a slightly charged surface with either excess positive or negative charge. In contrast to multivalent metal cations, which normally only condense DNA to undercharged particles, cationic polymers readily generate overcharged polymer−DNA particles (*18*). Since the charges on the dendrimer are concentrated to a very small area compared to the charges on the DNA, it is likely that the DNA cannot use all the charges on the dendrimer due to steric constraints, and therefore the particles will be overcharged. This is supported by the CD experiments that show, in contrast to the LD experiments which are less informative in this respect, that the CD spectrum for the pellet fraction resembles the CD for $r = 1.5$ rather than the CD for $r = 1$ (Figure 1B and Figure 3B). Similarly, the EtBr titration data show that the DNA in the pellet fraction displays a similar degree of ethidium exclusion as unfractionated dendrimer−DNA complexes at $r > 1$ (Figure 1C and Figure 3C). The presence of a nonzero LD signal for the pellet fraction could be explained by some small contamination of free DNA from the supernatant. This DNA would readily orient itself and give rise to LD, but it would not be as apparent in the CD or EtBr titration experiments.

Using the data for the ultracentrifugation experiments (Figure 2), we propose a model for the binding of dendrimers to DNA (Figure 6): at intermediate charge ratios (0−1), two fractions of differently condensed DNA coexist. The structure of the more condensed fraction is not clear, however the CD experiments give some information (vide infra). At higher charge ratios (>1), several of the condensed particles aggregate, aided by dendrimer "junctions" where one dendrimer binds to several different DNA strands or dendrimer−DNA complexes as proposed by Mitra et al. (*23*) as well as Örberg et al. (*32*). Formation of much larger complexes explains why, in the ultracentrifugation experiments, the pellet can no longer be redissolved at these charge ratios. Our binding model also gives an explanation to the results of other groups: Bielinska et al. found that condensation at low charge ratios was inefficient in protecting the DNA against nucleases and also inefficient in suppressing transcription (*19*), while Ottaviani et al. found that the change in melting profile upon condensation of DNA was negligible at $r < 1$ (*21*). Both of these seemingly negative results are due to the presence of a significant fraction of uncondensed DNA, which conceals the behavior of the condensed DNA fraction. This high degree of cooperativity might be due to the high charge density on the dendrimer surface in combination with the stiffness of the DNA helix: when a dendrimer has bound to the DNA, the helix cannot bend

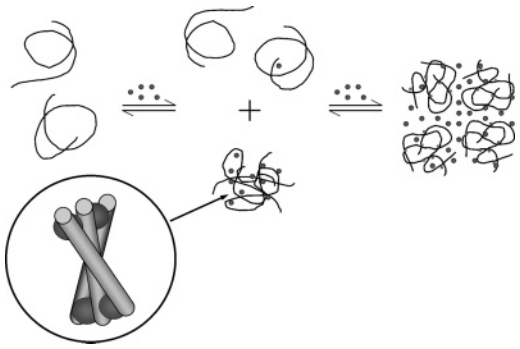

FIGURE 6: (A) Macroscopic cartoon model of DNA condensation by dendrimers. We propose two stages of compaction: (1) an intermediate stage (below charge neutrality) where relatively compact DNA globules or aggregates coexist with free or only loosely packed DNA coils and (2) (above charge neutrality) where the DNA is compacted into large aggregates consisting of several DNA globules with joining dendrimers in between. (B) Cartoon showing the principle of local chiral stacking of DNA helices evidenced from Ψ-type CD. Adjacent (B-form) DNA helices are close enough relative to each other to communicate a chiral bias (in the graph three DNA cylinders are arranged in a right-handed fashion). Interstitially located dendrimers (and sodium ions) contribute electrostatic attraction between the DNA helices, still allowing "cross-points" with steric proximity. The principle applies for the winding of adjacent DNA stretches in toroidal compact particles as well as in liquid-crystalline phases of dendrimer aggregates.

around it since it is slightly too small. Therefore, only one side of the dendrimer is "occupied" by the DNA. The other side provides a high concentration of positive charges, which readily attracts a second DNA stretch. These two DNA stretches close to each other in turn provide excellent binding sites for more dendrimers. As seen in Figure 5, condensing DNA with dendrimers has a very large impact on the level of gene expression, and the cooperativity is clearly manifested in that one fraction (supernatant) shows equal degree of transcription as uncondensed DNA, while the other fraction (pellet) is expressed to a much lower extent. By monitoring the luciferase production as a function of time, we are able to conclude that transcription is significantly delayed but not totally inhibited in the condensed pellet fraction. This is most likely due to that, as discussed by Bielinska et al. (*19*), the dendrimers inhibit formation of the transcriptional complex rather than the elongation of the transcript. After a while, the RNA polymerase happens to bind at the right place on the DNA and then transcription is initiated. Therefore, condensation with PAMAM dendrimers is not sufficient to permanently silence genes. This behavior is the same as that of histone proteins in chromatin, where both transcription and replication can proceed past the nucleosome (*33*, *34*). The regulatory effect of histones on gene expression is rather exhibited by the positioning of the nucleosomes, close to polymerase binding sites, than by strong binding between histones and DNA. Still, in our system we obtain a high level of discrimination between dendrimer-condensed and uncondensed DNA, mimicking the expression pattern in high and low-density chromatin regions in the cell nucleus.

Through LD, CD, DLS, and EtBr titrations, we have been able to characterize the structure of the dendrimer−DNA complexes (Figures 1, 3, and 4). As expected and as determined by LD, the complexes contain no long stretches of free DNA which could be oriented in a flow cell. In DLS, complexes appear relatively large and very heterogeneous, with average hydrodynamic radius of approximately 300 nm. This is the same trend as that observed by other groups and, due to the heterogeneity, some authors have suggested fractionation of complexes prior to, e.g., transfection experiments as a means to relate complex structure to function (*13*, *18*, *23*, *24*, *35*). The ethidium binding isotherms show that a surprisingly large part of the DNA, 70−80%, is still accessible for ethidium intercalation after condensation, even at high charge ratios. This result differs somewhat from those previously reported, where only 25−40% of the DNA was concluded to remain available for ethidium (*22*, *24*). This difference is in part explained by preparing complexes at different ionic strengths; Braun et al. prepared their complexes at a much lower ionic strength (10 mM) than was used in this study. Since the interaction is primarily electrostatic, a lower ionic strength should result in stronger binding between dendrimers and DNA and a higher degree of exclusion of ethidium in agreement with the variation observed and confirmed by independent experiments in our group (data not shown). By contrast, Chen et al. (*22*) prepared their complexes at 100 mM ionic strength which may be regarded very close to our 150 mM. Their calculated binding constant for uncondensed DNA is also very close to ours, as is the binding constant for charge ratio 0.5. For higher charge ratios, Chen et al. observe a considerably larger decrease than reported here in analogy with their higher degree of ethidium exclusion. The origin of this discrepancy is unclear.

A most remarkable observation about the dendrimer−DNA complexes, not previously reported, is the peculiar CD spectra they exhibit (Figure 1B and Figure 3B). This anomalous CD is also an observed characteristic of "polymer−salt-induced" Ψ-DNA, in which the DNA helices, by phase separation from a water−polymer solution, form a highly condensed structure (*36*). The origin of the anomalous CD can be related to a higher-order chiral structure with dimensions close to the wavelength of the incident light, and the chromophores close enough to couple with each other, as has been thoroughly investigated and explained by Keller and Bustamante (*30*). The simplest model for this higher-order structure is a cholesteric liquid crystalline phase in which the DNA helices are well aligned parallel with each other in a layer in which the direction of alignment is stepwise rotated, clockwise, or counterclockwise, with a given angle from one layer to the next, thereby creating a helical superstructure of DNA helices. As observed for DNA condensed with poly-L-lysine, another structure that also shows a Ψ-type CD spectrum is a DNA toroid, where the same effect is obtained locally as a result of a helical twist between close-lying DNA helices (*37*, *38*). Condensation of DNA with other cationic polymers, such as chitosan (*39*) and polyconidine (*31*), as well as the multivalent cations spermidine (*40*) and hexaammine cobolt (*5*), have also been associated with Ψ-type CD spectra. To our knowledge, though, this has never been reported for dendritic polymers, nor has Ψ-type CD been observed at the present relatively low salt concentrations. Sikorav et al. have found that spermidine and DNA may form a liquid chrystalline phase in equilibrium with a concentrated isotropic phase (*41*), and we also here see a similarity with our system. Many different condensing agents appear to cause DNA to adapt a toroidal

conformation, either by intermolecular collapse or by aggregation of several DNA molecules (*30*). Since the linearized plasmid DNA (~4300 bp) is too short to wind up as a single toroidal bundle with a diameter consistent with the persistence length of DNA (150 bp), and the DLS results show that the complexes in fact are larger (300 nm radius), the latter is most likely to occur in our system. With each complex consisting of several DNA molecules intertwined, a toroidal structure is easy to envisage, in which DNA coils lie in bundles with their helices slightly skewed relative to each other (structural principles shown in Figure 6).

Turning back to the analogy with chromatin, our findings could add to the understanding of the complexity of the regulation systems found in eucaryotic cell nuclei. Several important findings have been made regarding compaction of DNA by cationic 5.4 nm dendrimers. First, the DNA binding of the dendrimers is a cooperative process, yielding one fraction of highly compact complex, in which gene expression is turned off, while a remaining fraction of DNA behaves almost as uncomplexed DNA, both regarding structure and interactions with small molecules as well as enzymes. All spectroscopic studies support this conclusion indirectly, but it is the sedimentation results that definitely prove the cooperative behavior. The impact of cooperativity for gene regulation in the cell nucleus is a more effective silencing of transcription as is also shown here. Another important observation is the Ψ−type CD which implies that the dendrimer−DNA aggregates have a pronounced long-range structure but also a defined short-range structure in which DNA helices charge-neutralized by dendrimers and counterions (sodium) stack so close to each other that helix−helix contacts by diastereomeric preference lead to a superhelical structure. The compact and well-defined structure (like in a liquid crystal) can explain the observed cooperative behavior, such as for a phase transition. Cooperativity is also known in the gradual salt-assisted compaction of chromatin, where we may note that the transition between the 10 nm and the 30 nm fibers is associated with the stacking of nucleosomes into a superhelix.

ACKNOWLEDGMENT

We thank Dr. M. C. Grossel, Southampton University, for kindly providing us with dendrimers. We also thank our other collaborators in the NeoNuclei program. Further, we would like to thank Prof. J. Bergenholtz, Gothenburg University, for help with interpretation of the DLS data.

SUPPORTING INFORMATION AVAILABLE

Scatchard plots of ethidium titrations to dendrimer/DNA complexes, used to extract the data in Tables 1 and 2. This material is available free of charge via the Internet at http://pubs.acs.org.

REFERENCES

1. Mathews, C. K., and van Holde, K. E. (1996) *Biochemistry*, 2nd ed., The Benjamin/Cummings Publishing Company, Inc., Menlo Park.
2. Grewal, S. I., and Jia, S. (2007) Heterochromatin revisited, *Nat. Rev. Genet. 8*, 35−46.
3. Schiessel, H. (2003) The physics of chromatin, *J. Phys.: Condens. Matter 15*, R699−R774.
4. Gosule, L. C., and Schellman, J. A. (1976) Compact form of DNA induced by spermidine, *Nature 259*, 333−335.
5. Kankia, B. I., Buckin, V., and Bloomfield, V. A. (2001) Hexamminecobalt(III)-induced condensation of calf thymus DNA: circular dichroism and hydration measurements, *Nucleic Acids Res. 29*, 2795−2801.
6. Felgner, P. L., Gadek, T. R., Holm, M., Roman, R., Chan, H. W., Wenz, M., Northrop, J. P., Ringold, G. M., and Danielsen, M. (1987) Lipofection: a highly efficient, lipid-mediated DNA-transfection procedure, *Proc. Natl. Acad. Sci. U.S.A. 84*, 7413−7417.
7. DeRouchey, J., Netz, R. R., and Radler, J. O. (2005) Structural investigations of DNA-polycation complexes, *Eur. Phys. J. E:16*, 17−28.
8. Kabanov, V. A., Zezin, A. B., Rogacheva, V. B., Gulyaeva, Z. G., Zansochova, M. F., Joosten, J. G. H., and Brackman, J. (1998) Polyelectrolyte Behavior of Astramol Poly(propyleneimine) Dendrimers, *Macromolecules 31*, 5142−5144.
9. Brown, M. D., Schatzlein, A. G., and Uchegbu, I. F. (2001) Gene delivery with synthetic (non viral) carriers, *Int. J. Pharm. 229*, 1−21.
10. Zinchenko, A., and Chen, N. (2006) Compaction of DNA on nanoscale three-dimensional templates, *J. Phys.: Condens. Matter 18*, R453−R480.
11. Haensler, J., and Szoka, F. C., Jr. (1993) Polyamidoamine cascade polymers mediate efficient transfection of cells in culture, *Bioconjugate Chem. 4*, 372−379.
12. Kukowska-Latallo, J. F., Bielinska, A. U., Johnson, J., Spindler, R., Tomalia, D. A., and Baker, J. R., Jr. (1996) Efficient transfer of genetic material into mammalian cells using Starburst polyamidoamine dendrimers, *Proc. Natl. Acad. Sci. U.S.A. 93*, 4897−4902.
13. Tang, M. X., Redemann, C. T., and Szoka, F. C., Jr. (1996) In vitro gene delivery by degraded polyamidoamine dendrimers, *Bioconjugate Chem. 7*, 703−714.
14. Bielinska, A., Kukowska-Latallo, J. F., Johnson, J., Tomalia, D. A., and Baker, J. R., Jr. (1996) Regulation of in vitro gene expression using antisense oligonucleotides or antisense expression plasmids transfected using starburst PAMAM dendrimers, *Nucleic Acids Res. 24*, 2176−2182.
15. Yoo, H., Sazani, P., and Juliano, R. L. (1999) PAMAM dendrimers as delivery agents for antisense oligonucleotides, *Pharm. Res. 16*, 1799−1804.
16. Wada, K., Arima, H., Tsutsumi, T., Chihara, Y., Hattori, K., Hirayama, F., and Uekama, K. (2005) Improvement of gene delivery mediated by mannosylated dendrimer/alpha-cyclodextrin conjugates, *J. Controlled Release 104*, 397−413.
17. Huang, R. Q., Qu, Y. H., Ke, W. L., Zhu, J. H., Pei, Y. Y., and Jiang, C. (2007) Efficient gene delivery targeted to the brain using a transferrin-conjugated polyethyleneglycol-modified polyamidoamine dendrimer, *FASEB J. 21*, 1117−1125.
18. Tang, M. X., and Szoka, F. C. (1997) The influence of polymer structure on the interactions of cationic polymers with DNA and morphology of the resulting complexes, *Gene Ther. 4*, 823−832.
19. Bielinska, A. U., Kukowska-Latallo, J. F., and Baker, J. R., Jr. (1997) The interaction of plasmid DNA with polyamidoamine dendrimers: mechanism of complex formation and analysis of alterations induced in nuclease sensitivity and transcriptional activity of the complexed DNA, *Biochim. Biophys. Acta 1353*, 180−190.
20. Bielinska, A. U., Chen, C., Johnson, J., and Baker, J. R., Jr. (1999) DNA complexing with polyamidoamine dendrimers: implications for transfection, *Bioconjugate Chem. 10*, 843−850.
21. Ottaviani, M. F., Furini, F., Casini, A., Turro, N. J., Jockusch, S., Tomalia, D. A., and Messori, L. (2000) Formation of supramolecular structures between DNA and Starburst dendrimers studied by EPR, CD, UV, and melting profiles, *Macromolecules 33*, 7842−7851.
22. Chen, W., Turro, N. J., and Tomalia, D. A. (2000) Using Ethidium Bromide to probe the interactions between DNA and dendrimers, *Langmuir 16*, 15−19.
23. Mitra, A., and Imae, T. (2004) Nanogel formation consisting of DNA and poly(amido amine) dendrimer studied by static light scattering and atomic force microscopy, *Biomacromolecules 5*, 69−73.
24. Braun, C. S., Vetro, J. A., Tomalia, D. A., Koe, G. S., Koe, J. G., and Middaugh, C. R. (2005) Structure/function relationships of polyamidoamine/DNA dendrimers as gene delivery vehicles, *J. Pharm. Sci. 94*, 423−436.

25. Maksimenko, A. V., Mandrouguine, V., Gottikh, M. B., Bertrand, J. R., Majoral, J. P., and Malvy, C. (2003) Optimisation of dendrimer-mediated gene transfer by anionic oligomers, *J. Gene Med. 5*, 61−71.
26. Meltzer, A. D., Tirrell, D. A., Jones, A. A., Inglefield, D. M., Hedstrand, D. M., and Tomalia, D. A. (1992) Chain dynamics in poly(amidoamine) dendrimers: a study of carbon-13 NMR relaxation parameters, *Macromolecules 25*, 4541−4548.
27. Brown, T. A. (1998) *Gene cloning*, 3rd ed., Stanley Thornes (Publishers) Ltd, Cheltenham.
28. Norden, B., Kubista, M., and Kurucsev, T. (1992) Linear dichroism spectroscopy of nucleic acids, *Q. Rev. Biophys. 25*, 51−170.
29. Weiskopf, M., and Li, H. J. (1977) Poly(L-lysine)-DNA interactions in NaCl solutions: B to C and B to psi transitions, *Biopolymers 16*, 669−684.
30. Keller, D., and Bustamante, C. (1986) Theory of the interaction of light with large inhomogeneous molecular aggregates. II. Psi-type circular dichroism, *J. Chem. Phys. 84*, 2972−2980.
31. Skuridin, S. G., Gulyaeva, J. G., and Yevdokimov, Y. M. (2006) Structural Polymorphism of Liquid-Crystalline Dispersion of Double-Stranded DNA Complexed with Synthetic Polycations, *Mol. Biol. 40*, 961−969.
32. Orberg, M. L., Schillen, K., and Nylander, T. (2007) Dynamic light scattering and fluorescence study of the interaction between double-stranded DNA and poly(amido amine) dendrimers, *Biomacromolecules 8*, 1557−1563.
33. Lorch, Y., LaPointe, J. W., and Kornberg, R. D. (1987) Nucleosomes inhibit the initiation of transcription but allow chain elongation with the displacement of histones, *Cell 49*, 203−210.
34. Bonne-Andrea, C., Wong, M. L., and Alberts, B. M. (1990) In vitro replication through nucleosomes without histone displacement, *Nature 343*, 719−726.
35. Roessler, B. J., Bielinska, A. U., Janczak, K., Lee, I., and Baker, J. R., Jr. (2001) Substituted beta-cyclodextrins interact with PAMAM dendrimer-DNA complexes and modify transfection efficiency, *Biochem. Biophys. Res. Commun. 283*, 124−129.
36. Jordan, C. F., Lerman, L. S., and Venable, J. H. (1972) Structure and circular dichroism of DNA in concentrated polymer solutions, *Nat. New Biol. 236*, 67−70.
37. Shapiro, J. T., Leng, M., and Felsenfeld, G. (1969) Deoxyribonucleic acid-polylysine complexes. Structure and nucleotide specificity, *Biochemistry 8*, 3119−3132.
38. Haynes, M., Garrett, R. A., and Gratzer, W. B. (1970) Structure of nucleic acid-poly base complexes, *Biochemistry 9*, 4410−4416.
39. Yevdokimov, Y. M., Salyanov, V. I., Skuridin, S. G., Dembo, A. T., Platonov, Y. V., Il'ina, A. V., and Varlamov, V. P. (2000) Complexes between double-stranded DNA and chitosan can form cholesteric liquid-crystalline dispersions, *Dokl. Biophys. 373-375*, 47−49.
40. Becker, M., Misselwitz, R., Damaschun, H., Damaschun, G., and Zirwer, D. (1979) Spermine-DNA complexes build up metastable structures. Small-angle X-ray scattering and circular dichroism studies, *Nucleic Acids Res. 7*, 1297−1309.
41. Sikorav, J. L., Pelta, J., and Livolant, F. (1994) A liquid crystalline phase in spermidine-condensed DNA, *Biophys. J. 67*, 1387−1392.
42. McGhee, J. D., and von Hippel, P. H. (1974) Theoretical aspects of DNA-protein interactions: co-operative and non-co-operative binding of large ligands to a one-dimensional homogeneous lattice, *J. Mol. Biol. 86*, 469−489.

BI7017199